ISRG Journal of Economics, Business & Management (ISRGJEBM)

ISRG PUBLISHERS

Abbreviated Key Title: Isrg J Econ Bus Manag

ISSN: 2584-0916 (Online)

Journal homepage: https://isrgpublishers.com/isrgjebm/

Volume – IV Issue - II (March-April) 2026

Frequency: Bimonthly

Comparative Assessment of Isobase and Polynomial Trend Surface Methods for Paleo-Shoreline Prediction in Lebanon.

Jean A. Doumit

Lebanese University, Faculty of Letters and Human Sciences, Department of Geography, Geospatial Lab.

| **Received:** 10.03.2026 | **Accepted:** 15.03.2026 | **Published:** 19.03.2026

***Corresponding author:** Jean A. Doumit

Abstract

The emergence of Lebanon during the Miocene reflects the combined effects of regional tectonic uplift and sea-level fluctuations along the Levant margin. This study applies geomorphometric methods to reconstruct paleotopography and predict paleoshoreline positions using SRTM30 PLUS Digital Elevation Model data. Two independent approaches were evaluated: isobase surface construction from Strahler-ordered valley networks and polynomial trend surface modeling based on regression analysis of elevation data. Four successive orders of isobase and trend surfaces were generated and compared.

Zero-elevation contours extracted from each surface were interpreted as paleoshorelines and analyzed using correlation statistics (R^2), hypsometric classification, fractal dimension, and sinuosity indices. The modeled shorelines were validated against the spatial distribution of documented marine deposits and fossiliferous sites in Lebanon.

Results indicate that lower-order surfaces closely resemble present-day topography, whereas higher-order surfaces reflect progressive regional emergence. Although higher-order trend and isobase surfaces appear statistically similar due to terrain smoothing, shoreline geometry and spatial validation indicate that isobase-derived reconstructions better preserve morphostructural complexity and align more closely with marine depositional evidence. The study confirms that isobase geomorphometry provides a more reliable framework for paleoshoreline prediction in tectonically active continental margins.

Keywords: *Paleo-shorelines, Isobase, Trend surfaces, DEM, Geomorphometry*

1. Introduction

Shorelines mark the boundary between terrestrial and marine environments, and displacements between paleoshoreline locations indicate vertical motions over geological time (Veevers & Morgan, 2000; Heine et al., 2010).

Heine et al. (2015) evaluated Cretaceous and Cenozoic paleoshorelines from two independent global paleogeographic atlases: those of Smith et al. (1994) and Golonka et al. (2006). They also compared the extent of flooding with fossil locations.

DOI: 10.5281/zenodo.19107119

The Miocene rock succession in Lebanon has been divided into a marine (reefal) and a conglomeratic-lacustrine unit (Dubertret, 1975). The Levant coastal area and shelf became emergent in the Early Miocene and the end Miocene period (Hawie et al., 2014)

Saint-Marc (1970) ascribes the "Falaise de BLANCHE" to an Aptian age based on the identification of benthic foraminifers and calcareous algae.

Dalla Vecchia et al. (2001) mention four main fossiliferous sites in Lebanon: Hakel, Hjoula, Nammoura, and Sahel Aalma (Garassino, 1995).

Maksoud et al. (2014) studied benthic deposits in the Jezzine region and cited Dubertret, who described macrofossils (Dubertret, 1955, 1963; Dubertret & Vautrin, 1937).

All the research studies listed above examine benthic deposition in Lebanon. Our paper relies on the geomorphometry of Lebanese bathymetry and topography to predict the positions of older sea-level shorelines using two methods: the first based on the valley-order network, and the second on regression functions.

As per Dury (1952), Filosofov (1960), and Pannekoek (1967), Isobase maps express a relationship between valley order and topography. The valley order is one of Strahler's (Strahler, 1952), in which streams of similar orders are associated with similar geological ages (Golts & Rosenthal, 1993). Each isobase order surface is related to similar erosional stages and tectonic events (Golts and Rosenthal, 1992, 1993).

Powell (1875) defined the concept of Isobase maps as a level "below which the drylands cannot be eroded", several authors have agreed that an isobase map can be defined according to different geological and temporal conditions (Powell, 1875; Davis, 1902; Mackin, 1948; Penck, 1953; Quirk,1996).

The word " isobase surfaces " was used by Filosofov (1960, 1970, 1975) and Grohmann et al. (2007); other authors used different alternative words, such as base level map (Grohmann et al., 2011), base-level surfaces (Zuchiewicz & Oszczypko, 2008), base surface (Ufimtsev et al., 2009), sub envelopes map (Stearns, 1967; Raczkowski et al., 1984; Hack, 1960), and streamline surface map of Dury (1952) and Pannekoek (1967).

Leverington et al. (2002), in their paper entitled A GIS method for reconstruction of late quaternary landscapes from isobase data and modern topography, used isobases as lines of equal uplift and applied them to marine terraces and Holocene shorelines (Leverington et al., 2002).

In this paper, in addition to Isobase maps, we used trend-surface analysis to analyze planation surfaces and to synchronize shorelines of older sea levels. (Svensson 1950).

Like other statistical methods, trend surface analysis in a GIS environment requires systematic data collection and sampling, preferably in a grid pattern.

This paper describes methods for constructing isobases and trend surfaces from DEMs to extract shorelines at older sea levels, compares the resulting isobases and trend surfaces, and validates them against the spatial locations of marine deposits and fossils.

This study does not address geological or geophysical issues; it only tests geomorphometric methods for predicting paleo shorelines.

2. Materials and Methods

As per Buchbinder and Zilberman (1997), during the Early Miocene, the Levant margin and the Lebanese territory became emergent (Buchbinder & Zilberman, 1997).

Much research indicates that the end of the Miocene period is marked by the rapid emergence of Mount Lebanon above sea level, leading to the deposition of marine Pliocene sediments. (Haq et al.1988, Dubertret 1975; Elias 2006).

To predict the positions of paleo-shorelines from isobase and trend surfaces during the stages listed above, we used the open-source Shuttle Radar Topographic Mission (SRTM) 30 PLUS DEMs, with a spatial resolution of approximately 900m, to extract and classify valley networks (Becker & Sandwell, 2007).

The geomorphometry analysis consists of three steps: defining valley orders (stream orders), preparing isobase maps, and constructing trend surfaces directly from the DEM.

Strahler valley order designates the relative position of valley segments. Filosofov (1960) assigns a relative geological age to each valley order; therefore, isobase maps reveal various morphological features that could be related to different geological stages.

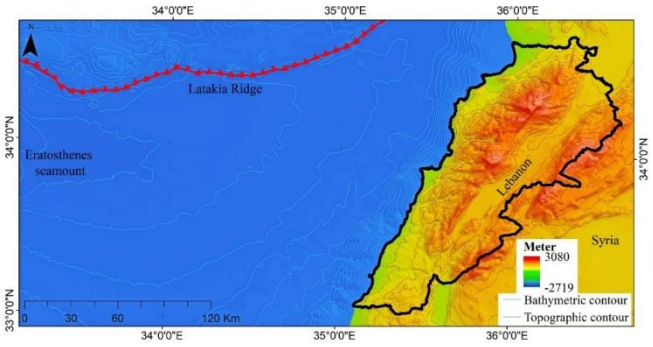

Fig.1: Study area map of the Levantine basin and the Lebanese onshore.

According to Filosofov (1960), the isobase surface is the hypothetical plane formed by interpolating the valley profiles of similar order. The streambeds of the valleys define the erosional base surface.

The elevation of an isobase line is retrieved from the DEM along valleys of similar order and is related to similar erosional stages and tectonic events in crustal movement.

As per Gary et al. (1973), isobase surfaces are a useful tool for deciphering young tectonic processes (Gary et al., 1973). For the tectonic interpretation of an isobase map, we should take into consideration:

The sharp deviation toward isobase lines indicates tectonic dislocations or lithological changes, and the compression of isobase lines could indicate steeply dipping strata, fracturing, or faulting.

The valley extraction requires a hydrological correction of the SRTM Digital Elevation Models; the entire process for creating and ordering the drainage network is depicted in Figure 2.

For the identification of the Strahler valley order for each stream in the valley network (Strahler, 1952).

DOI: 10.5281/zenodo.19107119

First, the flow direction raster is calculated after DEM depression filling; then, from the generated flow direction raster, a flow accumulation raster is created.

From both the raster flow direction and the raster flow accumulation, the Ordered Stream is created and converted from a raster to a vector representation.

Using stream heights obtained from the DEM and elevation vertices generated for each Strahler-ordered valley network, isobase surfaces of selected orders can be constructed (Figure 2).

The elevation of intersection points between drainage and contours was used to create vertex points.

The elevations at the vertices of the 1st, 2nd, 3rd, and 4th valley orders were interpolated using the Regularized Splines with Tension method to form four isobase surfaces: 1, 2, 3, and 4. The valley orders of 5th, 6th, and 7th were excluded from the study due to poor spatial distribution of elevation points and the inability to perform surface interpolation.

Interpolated isobase surfaces are smoother and simpler than the original topography, highlighting well-defined terrain inflections and fault lines, and are useful as a structural background for seismic survey investigations (Golts and Rosenthal 1993).

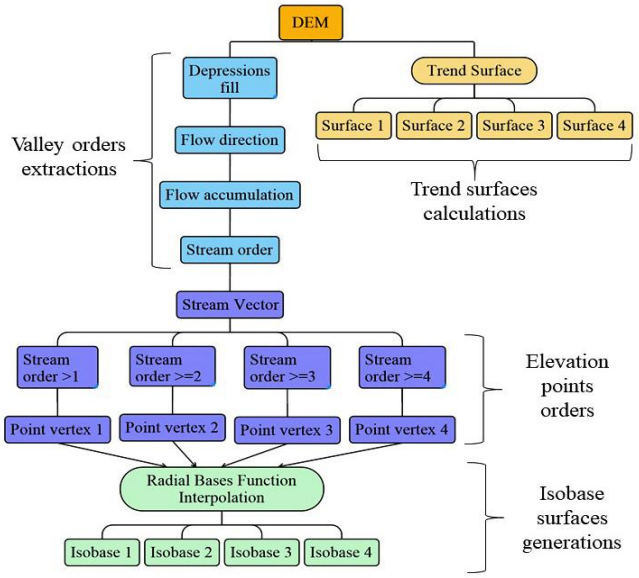

Fig.2: The geoprocessing workflow of the Isobase and trend surface construction.

Trend surface models are bivariate regression models with two independent variables, the coordinates X and Y and a dependent variable Z, the first order is a linear regression function, the 2nd, 3rd, …, or nth order is polynomial functions with our study dealing with terrain elevations the regression function of the first order reversed to be the surface of the 4th order very similar the recent terrain equation 1 the second and third polynomial functions became the 3rd. The 2nd trend surface emerges; hence, the 1st polynomial order serves as the 1st trend surface, with very complex terrain and very similar to the real elevation distributions (the DEM) calculated by equation 4 (Krumbein, 1956).

For the calculation of trend surfaces, progressive expansions of linear, quadratic, and cubic polynomial functions have been used as follows (Davis, 1986; Unwin, 1975):

The linear trend surface of the fourth order:

$$Z = a + bY + cX \quad (1)$$

The bilinear trend surface of the third order:

$$Z = a + bY + cX + dXY \quad (2)$$

The trend surface of the second order:

$$Z = a + bY + cY^2 + dX + eX^2 + fXY \quad (3)$$

The trend surface of the first order:

$$Z = a + bY + cY^3 + eX + fXY + gXY^2 + hX^2 + iX^2Y + jX^3 \quad (4)$$

Trend surface modeling is applied in a geographic information context on SRTM-DEM. This approach will draw the global trend of elevation distribution as surfaces of different orders. The trend surface spatial distribution becomes more complex as the order increases.

3. Results and Discussions

The study area's valley network, classified using the Strahler method, consisted of 7 orders, as shown in Figure 3.

The Litani, El Bared, Abou Ali, and Ibrahim rivers were classified as a 3rd-order valley. Figure 3 shows straight-line valleys in the western part of the study area; these are artifacts of low DEM spatial resolution, are far from the Lebanese shoreline, and do not affect our study.

The generated Strahler valley orders of Figure 3 are used for the interpolation of the Isobase surfaces; the 5th,6th, and 7th orders are excluded from the interpolation because they do not cover the Lebanese territories, which are within the Levantine basin.

The Isobase surfaces constructed from 2nd- and 3rd-order valleys show the best spatial distribution and interpolation results. In the Isobase surfaces of the 3rd and 4th orders, all morpho structures (ridges and valleys) can still be identified, though with less detail.

The constructed Isobase surfaces of the 1st, 2nd, 3rd, and 4th orders for figures 4b, d, f, and h help identify uplifted areas and the amplitude and crustal movement (Raczkowski et al., 1984; Jedlička et al., 2015; Doumit, 2017).

The Isobase surfaces of 1st and 2nd orders were considered too close to resemble the DEM's recent topography; the Isobase surface of the 3rd order showed dominant fault- and fold-related undulations (Jedlička et al., 2015).

Local anticlinal structures are characterized by short distances between isobase contour lines (Filosofov, 1970); isobases run straight and parallel to each other within homoclinal structures (Zuchiewicz, 1989), while changes in the isobase surface indicate possible fault locations (Shahzad & Gloaguen, 2011).

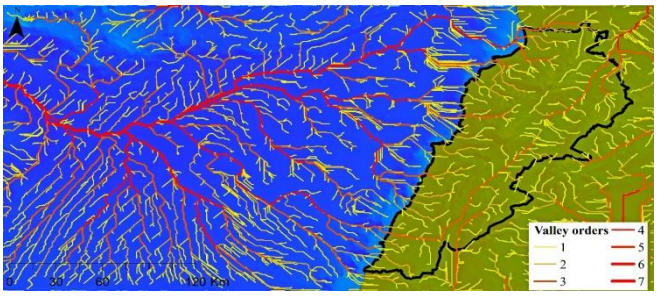

Fig.3: Strahler valley order of the study area

Figure 4a shows the topographic surface and the recent shoreline. Figure 4b shows the 1st-order isobase surface, which simplifies

DOI: 10.5281/zenodo.19107119

terrain elevations by obscuring the Barouk Mountains and smoothing the Saninne and Qornet Es Sawda Mountains.

Also, Figure 4b shows the emergence of the coastal cities of Sour, Beirut, and Tripoli. In Figure 4d, the second-order isobase surface for Sannine and the Qornet Es Sawda Mountains merged into a single hill, and most of the Lebanese coastal plain was submerged.

The third-order Isobase surface in Figure 4f shows the complete disappearance of the Mount Lebanon chain and the emergence of the southern part of the country, including the cities of Beirut, Byblos, and Tripoli.

The 4th-order Isobase surface showed that approximately 80% of Lebanese territory has emerged, with the disappearance of the Yammouneh Fault and high onshore deformation in the Hermel region.

We note that the modeling of Isobase surfaces in our study stops at the 4th-order Isobase, which does not prove that the emergence was stopped. As mentioned above, this paper is concerned only with Isobase and trend-surface physiography, and with predicting paleoshoreline positions.

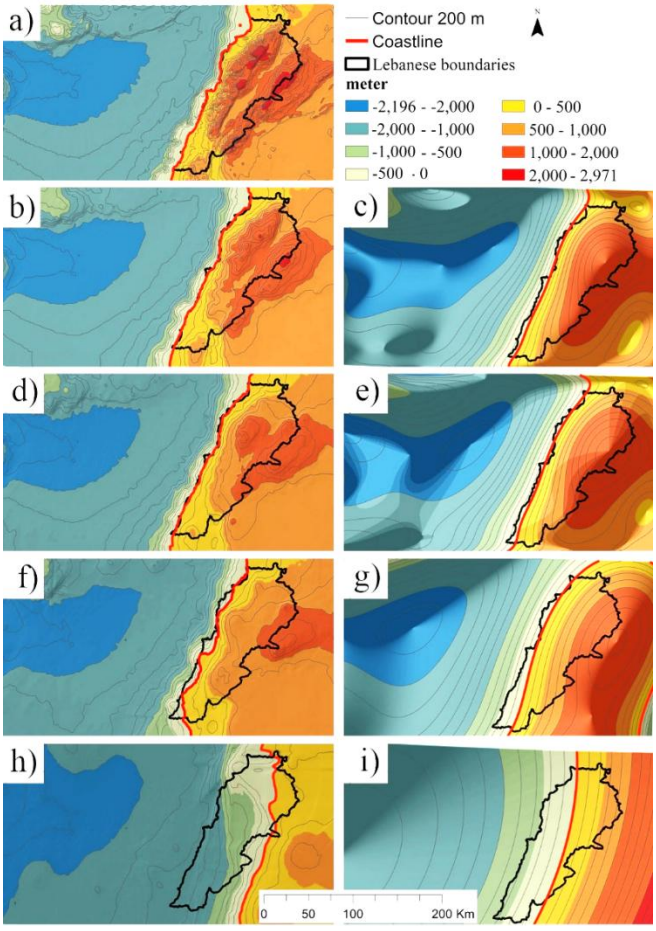

Fig.4: The following figure illustrates Isobase and trend surfaces with intervals of 200 meters; a) the SRTM Digital Elevation Model, b) Isobase surface of the 1st order, c) Trend surface of the 1st order, d) Isobase surface of the 2nd order, e) Trend surface of the 2nd order, f) Isobase surface of the 3rd order, g) Trend surface of the 3rd order, h) Isobase surface of the 4th order, i) Trend surface of the 4th.

Figures 4c and 4e of the Trend surfaces of the first and second orders are very similar. The terrain is very smooth, and there is only one closed contour loop joining the Lebanon and Anti-Lebanon mountains. The shoreline is straight, indicating that the Bays of Jounieh and Akkar have not emerged. The shoreline in Figure 4g of the third-order Trend surface became convex, and the terrain is more simplified, trending eastward. Contrary to the third-order trend surfaces, the fourth-order trend surface, with concave contour lines in the form of a depression, produced an arc shoreline that divided Lebanon into two parts: a western emergent one and an eastern slope rising approximately 1000 meters.

Visually, Isobase surfaces are unlike Trend surfaces; they are rougher and more complex, preserving the terrain's geological and geomorphological structures. Otherwise, Trend surfaces are very smooth, exaggerating terrain and obscuring geological and geomorphological structures.

The Morphometric analysis of the Isobase and Trend surfaces is expressed in eight hypsometric intervals: four representing bathymetric depth and the other representing terrain elevation, as shown in the legend of Figure 4.

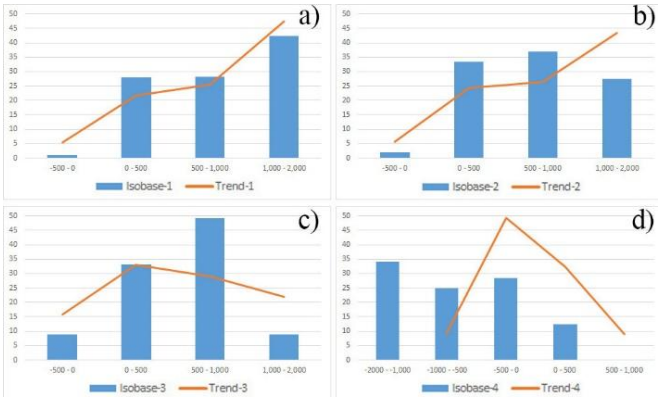

Fig.5. hypsometric histograms of the area percentage occupied by the elevation intervals of Isobase and trend surface, a) first-order Isobase and Trend surfaces elevation interval, b) second-order Isobase and Trend surfaces elevation interval, c) third-order Isobase and Trend surfaces elevation interval, d) fourth-order Isobase and Trend surfaces elevation interval.

After cropping the Isobase and Trend surfaces within Lebanese boundaries and classifying them by the hypsometric interval shown in Figure 5, the raster datasets were converted to vector format for the calculations.

Figure 5 shows the variations in areas in each order; the increase in emerging area is high in the third and fourth orders of Isobase surfaces, and the decrease in the onshore area from the 1st order to the 4th order, with the disappearance of the elevation interval of 500-1000.

From the results of figure 5 we can summarize that in the 1st, 2nd and 3rd orders the emergence was in an interval of depth between -500 to 0, it means the water covers the Lebanese territories situated under 500 meters above the Sea level, otherwise in Isobase surface of the 4th order, the water covers the territories at the elevations under 2000 meters above the Sea level.

The peak in the area percentage of the Isobase surface in the 2nd-order histogram is shown in Figure 5b and begins at the 500-1000 interval. We mean by the peak the transition point from an increase in area percentage to its decrease.

The peak in the area percentage trend surface occurs in the third-order figure 5c at the 0-500 interval.

DOI: 10.5281/zenodo.19107119

From these visual and quantitative analyses, the simplicity of the Trend surfaces is higher than that of the Isobase surfaces, and this simplicity strongly influences cartographic generalization; hence, we can deduce that Isobase surfaces belong to big-scale maps, whereas Trend surfaces belong to small-scale maps.

Table 1: Correlation matrix with R^2 values of the original DEM, the Isobase, and Trend Surfaces.

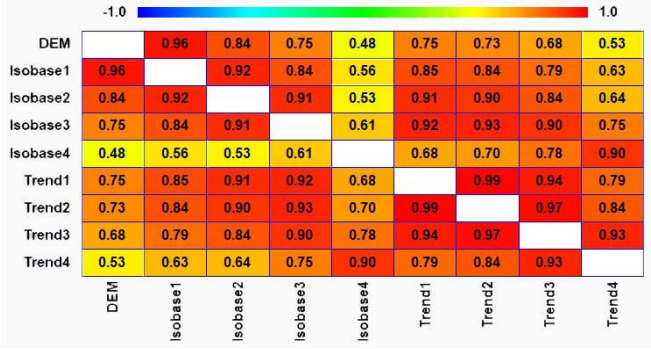

A regression analysis of Isobase and Trend Surfaces was made to understand similarity between them, table 1of the R^2 values shows a decrease of similarity between Isobase surfaces and the DEM with the decrease in orders, a descendent ordering in the R^2 values of the Isobase of the 1st and 2nd orders correlation with the DEM and all Isobase and Trend surfaces, this result proves the high similarity between Isobase of the 1st and 2nd orders with the recent Terrain.

Contrary to the R^2 values for Isobase columns in Table 1, the Isobase of the fourth order, with ascending values, shows a trend more like the Isobase surfaces, resulting in smoother morphological forms (Figure 4).

High R2 values of the 1st, 2nd, and 3rd orders of the trend surfaces with the Isobase surfaces of the 1st, 2nd, and 3rd orders and their proportionality to the R2 values of the Isobase of the 4th order, the trend surface of the 3rd order correlates with the recent relief expressed by the DEM.

From the result of Table 1, we can conclude that the 1st,2nd, and 3rd orders of Isobase and Trend surfaces are very similar to the DEM.

The high correlation between the Isobase surfaces of the 4th order and the Trend surfaces is related to the terrain smoothness. It leads to the disappearance of morphological structures (faults and flexures).

It is well known that a contour line is a line joining points with the same elevation, and elevation zero is a reference to the mean Sea level. We extracted contour lines at zero elevation for all isobases and Trend surfaces to use as shorelines (Figure 7).

Isobase shorelines of the 1st,2nd, and 3rd orders are close between Tripoli and Arida to the Syrian borders, between Nahr Ibrahim and Jbeil, and in the Damour region.

Table 2 of the shorelines' geometrical characteristics shows an increase in fractal dimension values with increasing Isobase order, and as noted above, the Isobase surface became smoother with increasing order. This result proves there is no relation between the smoothness of Isobases surfaces and the fractal dimensions of the shorelines.

The fractal dimensions of the Trend surface shorelines do not change with Trend surface order; they are approximately 1, indicating that the shorelines are approximately straight lines for all surfaces. Like the fractal dimension, the sinuosity of the shorelines increases with the increase in surface orders, and the sinuosity is not related to the smoothness and simplicity of Isobase surfaces.

Table 2: Isobase and Trend shorelines geometrical characteristics.

Shoreline Type	Length-km	Fractal Dimension	Sinuosity
Recent	324	1.06	1.71
Isobase-1	198	1.01	1.04
Isobase-2	198	1.01	1.04
Isobase-3	206	1.02	1.12
Isobase-4	105	1.04	1.19
Trend 1	189	1.00	1.00
Trend 2	187	1.00	1.00
Trend 3	186	1.00	1.01
Trend 4	150	1.00	1.01

Because Isobase-generated shorelines are independent of surface roughness and depend only on terrain elevations, their spatial positions and geometric characteristics are more realistic and better represent paleogeography than those generated from Trend surfaces, which exhibit a high degree of cartographic generalization.

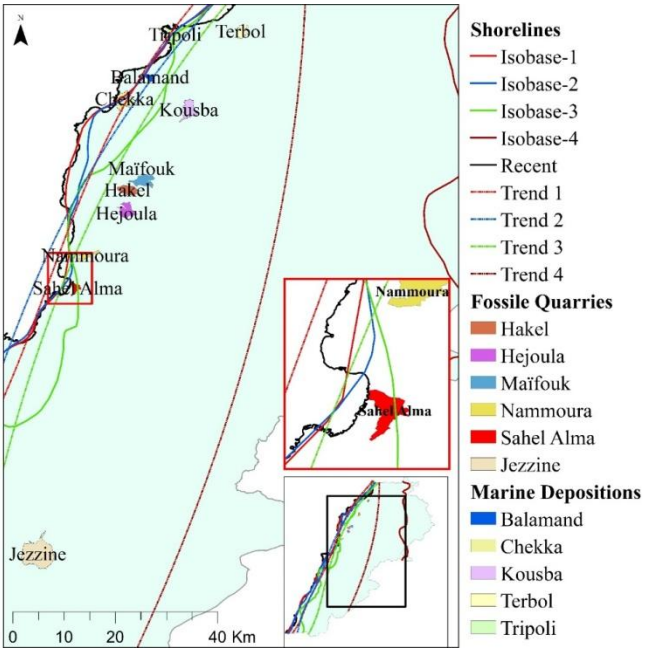

Fig.7. Isobase and Trend surfaces shorelines with Marine depositions and fossil locations.

To validate the generated isobase and trend surfaces, shorelines with marine deposition are used.

In their study of the sedimentology and stratigraphic evolution of Northern Lebanon, Hawie et al. (2013) spoke in detail about marine depositional environments prevailing in the Turonian to Late Miocene in Balamand, Chekka, Kousba, Terbol, and Tripoli, as our study is only dealing with the geomorphometry, terrain physiography, and the prediction of shoreline position. We will

DOI: 10.5281/zenodo.19107119

compare the locations of marine depositions reported by Hawie et al. (2013) with those of fossil quarries reported by Dalla Veccchia et al. (2001) and with the generated Shorelines based on Isobase and Trend surfaces.

The Late Cretaceous-age preserved fossil assemblage comprises four main fossiliferous sites in Lebanon: Hakel, Hajoula, Nammoura, and Sahel Aalma.

The Sahel Aalma site is the youngest and is of late Santonian age (Garassino, 1995). Figure 7 shows that isobase 4 crosses the Sahel Alma region; here, the Sahel Alma in the fourth-order isobase surface has emerged beneath the sea in the late Santonian age.

The Nammoura site is regarded as late middle Cenomanian (Dalla Vecchia & Venturini, 1999) and is on the shoreline of the isobase surface 4.

The ages of the Hakel and Hjoula are early Cenomanian (Saint Marc, 1974); both sites are within the Isobase and fourth-order trend surfaces.

The shoreline of the Isobase surface of the 3rd order and the Trend surfaces of the 1st and 2nd orders show the emergence of Chekka, Balamand, and half of Tripoli city.

The shorelines of the Isobase and Trend surfaces of the 4th order are shifted eastward, showing that Kousba and Terbol emerged.

Based on the spatial locations of shorelines and marine environmental depositions, we can classify shorelines into two classes.

The first class contains the shorelines of Isobase and Trend surfaces of the 1st, 2nd, and 3rd orders, including the marine depositions of Sahel Alma, Chekka, Balamand, and Tripoli.

The second class, Isobase and Trend surface shorelines of the 4th order, including the marine deposition locations of Hejoula, Hakel, Maifouk, Kousba, and Terbol.

The results, in addition to the generation of the GIS paleo-topography database expressed in Isobase and Trend surface orders, the prediction of paleo-shoreline positions, and the validation of their spatial positions against marine deposits, demonstrate that Isobase-based shorelines are more reliable than those generated from Trend Surfaces.

4. Conclusion

This study demonstrates the effectiveness of DEM-based geomorphometric techniques for reconstructing paleo-topography and predicting paleo-shorelines in Lebanon. The comparison between Isobase and Trend surface modeling reveals clear methodological contrasts. Trend surfaces provide generalized, smooth representations of elevation patterns, suitable for regional-scale approximations. In contrast, Isobase surfaces derived from valley-order networks retain morpho-structural features and better reflect tectonic and erosional controls.

Quantitative analyses and validation using marine depositional environments and fossil sites confirm that Isobase-derived shorelines, particularly those from second- and third-order surfaces, yield more realistic paleogeographic reconstructions. Fractal dimension and sinuosity metrics further support the greater geomorphic reliability of Isobase shorelines compared to Trend-generated shorelines.

The spatial resolution of DEM data remains a limiting factor in surface accuracy. Future work incorporating higher-resolution topographic and bathymetric datasets will improve shoreline precision and enhance paleo-geographic modeling. Overall, Isobase geomorphometry represents a robust and reliable approach for paleo-shoreline reconstruction along tectonically active margins such as the Levant Basin.

References

1. Becker, J. J., & Sandwell, D. T. (2007). *SRTM30 PLUS: Data fusion of SRTM land topography with measured and estimated seafloor topography (Version 3.0)*. Scripps Institution of Oceanography. http://topex.ucsd.edu/WWW_html/srtm30_plus.html
2. Buchbinder, B., & Zilberman, E. (1997). Sequence stratigraphy of Miocene–Pliocene carbonate-siliciclastic shelf deposits in the eastern Mediterranean margin (Israel): Effects of eustasy and tectonics. *Sedimentary Geology, 112*(1-2), 7–32. https://doi.org/10.1016/S0037-0738(97)00030-9
3. Heine, C., Yeo, L. G., & Müller, R. D. (2015). Evaluating global paleoshoreline models for the Cretaceous and Cenozoic. *Australian Journal of Earth Sciences, 62*(3), 275–287. https://doi.org/10.1080/08120099.2015.1018321
4. Dalla Vecchia, F. M., & Venturini, S. (1999). The Middle Cenomanian Lagerstätte of Al Nammoura (Kesrouane Caza, N. Lebanon). *Rivista del Museo Civico di Scienze Naturali di Bergamo "E. Caffi", 20*, 75–78. https://www.researchgate.net/publication/285032822
5. Dalla Vecchia, F. M. (1998). New observations on the osteology and taxonomic status of *Preondactylus buffarinii* Wild, 1984 (Reptilia, Pterosauria). *Bollettino della Società Paleontologica Italiana, 36*(3), 355–366. https://biostor.org/reference/140683
6. Davis, J. C. (1986). *Statistics and data analysis in geology* (2nd ed.). John Wiley & Sons.
7. Davis, W. M. (1902). Base level, grade, and peneplain. *The Journal of Geology, 10*(1), 77–111. https://doi.org/10.1086/620984
8. Doumit, J. A. (2017). Discovery of crustal movements areas in Lebanon: A study of Geographical Information Systems. *Bulletin of Environment, Pharmacology and Life Sciences, 6*(5), 48–52. http://www.bepls.com/april2017/8.pdf
9. Dubertret, L. (1975). Introduction à la carte géologique au 1/50000 du Liban. *Notes et Mémoires sur le Moyen-Orient, 23*, 345–403.
10. Dubertret, L., & Vautrin, H. (1937). Révision de la stratigraphie du Crétacé du Liban. In L. Dubertret (Ed.), *Contributions à l'étude géologique de la côte libano-syrienne* (Vol. 2, pp. 43–85). Haut-Commissariat de la République Française en Syrie et au Liban.
11. Dubertret, L. (1934). Première partie. La carte géologique au millionième de la Syrie et du Liban. *Revue de Géographie Physique et de Géologie Dynamique,*

DOI: 10.5281/zenodo.19107119

6(4), 269–318. https://doi.org/10.1016/S1765-2901(34)80016-1

12. Dubertret, L. (1947). Aperçu de la géographie physique du Liban, de l'Anti-Liban et de la Damascène. *Notes et Mémoires sur le Moyen-Orient, 4*, 191–226.
13. Dubertret, L. (1955). *Notice explicative de la Carte géologique du Liban au 1:200 000*. Ministère des Travaux Publics.
14. Dubertret, L. (1963). Liban et Syrie: Chaîne des grands massifs côtiers et des confins à l'Est. In L. Dubertret (Ed.), *Liban, Syrie, Jordanie. Lexique Stratigraphique International* (Vol. III, Fasc. 10 c1, pp. 7–155).
15. Dury, G. H. (1952). *Map interpretation*. Arnold.
16. Elias, A. (2006). *Le chevauchement de Tripoli-Saida: Croissance du Mont-Liban et risque sismique* [Doctoral dissertation, Institut de Physique du Globe de Paris]. https://www.theses.fr/2006IPGP0010
17. Filosofov, V. P. (1970). Maps of isobases and residual relief. In *Application of geomorphic methods in structural investigations* (pp. 43–52). NEDRA.
18. Filosofov, V. P. (1960). *Brief guide to morphometric methods in search of tectonic structures*. Saratov University Publishing House.
19. Filosofov, V. P. (1975). *The basis of the morphometric method in search of tectonic structures*. Saratov University Publishing House.
20. Garassino, A. (1994). The macruran decapod crustaceans of the Upper Cretaceous of Lebanon. *Paleontologia Lombarda, 3*, 1–40.
21. Gary, M., McAfee, R., & Wolf, C. (1973). *Glossary of geology* (2nd printing). American Geological Institute.
22. Golonka, J., Krobicki, M., Pajak, J., Van Giang, N., & Zuchiewicz, W. (2006). *Global plate tectonics and paleogeography of Southeast Asia*. AGH University of Science and Technology.
23. Golts, S., & Rosenthal, E. (1993). A morphotectonic map of the northern Arava in Israel, derived from isobase lines. *Geomorphology, 7*(4), 305–315. https://doi.org/10.1016/0169-555X(93)90060-F
24. Golts, S., & Rosenthal, E. (1992). Morphotectonic methods to infer groundwater flow under conditions of scarce hydrogeological data: The case of northern Arava, Israel. *Hydrogeology Journal, 1*(1), 5–19. https://doi.org/10.1007/s100400050245
25. Grohmann, C. H., Riccomini, C., & Alves, F. M. (2007). SRTM-based morphotectonic analysis of the Poços de Caldas Alkaline Massif, southeastern Brazil. *Computers & Geosciences, 33*(1), 10–19. https://doi.org/10.1016/j.cageo.2006.05.002
26. Grohmann, C. H., Riccomini, C., & Chamani, M. A. C. (2011). Regional-scale analysis of landform configuration with base-level (isobase) maps. *Hydrology and Earth System Sciences, 15*(5), 1493–1504. https://doi.org/10.5194/hess-15-1493-2011
27. Hack, J. T. (1960). Interpretation of erosional topography in humid temperate regions. *American Journal of Science, 258A*, 80–97. https://doi.org/10.2475/ajs.258.A.80
28. Haq, B. U., Hardenbol, J., & Vail, P. R. (1988). Mesozoic and Cenozoic chronostratigraphy and eustatic cycles. In C. K. Wilgus et al. (Eds.), *Sea-level changes: An integrated approach* (SEPM Special Publication No. 42, pp. 71–108). SEPM Society for Sedimentary Geology.
29. Hawie, N., Deschamps, R., Nader, F., Gorini, C., Müller, C., Desmares, D., Hoteit, A., Granjeon, D., Montadert, L., & Baudin, F. (2013). Sedimentological and stratigraphic evolution of northern Lebanon since the Late Cretaceous: Implications for the Levant margin and basin. *Arabian Journal of Geosciences, 7*(4), 1323–1349. https://doi.org/10.1007/s12517-013-0914-5
30. Heine, C., Müller, R. D., Steinberger, B., & DiCaprio, L. (2010). Integrating deep Earth dynamics in paleogeographic reconstructions of Australia. *Tectonophysics, 483*(1-2), 135–150. https://doi.org/10.1016/j.tecto.2009.08.028
31. Horton, R. E. (1945). Erosional development of streams and their drainage basins: Hydrophysical approach to quantitative morphology. *Geological Society of America Bulletin, 56*(3), 275–370. https://doi.org/10.1130/0016-7606(1945)56[275:EDOSAT]2.0.CO;2
32. Jedlička, K., Sládek, J., & Šilhavý, J. (2015). Semiautomatic construction of isobase surfaces: A case study from the central Western Carpathians. *Computers & Geosciences, 78*, 50–61. https://doi.org/10.1016/j.cageo.2015.02.012
33. Krumbein, W. C. (1956). Regional and local components in facies maps. *AAPG Bulletin, 40*(9), 2163–2194. https://doi.org/10.1306/5CEAE5B8-16BB-11D7-8645000102C1865D
34. Leverington, D. W., Teller, J. T., & Mann, J. D. (2002). A GIS method for reconstruction of late Quaternary landscapes from isobase data and modern topography. *Computers & Geosciences, 28*(5), 631–639. https://doi.org/10.1016/S0098-3004(01)00069-0
35. Mackin, J. H. (1948). Concept of the graded river. *Geological Society of America Bulletin, 59*(5), 463–512. https://doi.org/10.1130/0016-7606(1948)59[463:COGR]2.0.CO;2
36. Maksoud, S., Granier, B., Azar, D., Gèze, R., Paicheler, J. C., & Moreno-Bedmar, J. (2014). Revision of "Falaise de Blanche" (Lower Cretaceous) in Lebanon, with the definition of a Jezzinian Regional Stage. *Carnets de Géologie, 14*(18), 401–427. https://doi.org/10.4267/2042/54359
37. Pannekoek, A. F. (1967). Generalized contour maps, summit level maps, and streamline surface maps as geomorphological tools. *Zeitschrift für Geomorphologie, 11*, 169–182.

DOI: 10.5281/zenodo.19107119

38. Penck, W. (1953). *Morphological analysis of landforms: A contribution to physical geology* (H. Czech & K. C. Boswell, Trans.). Macmillan.

39. Powell, J. W. (1875). *Exploration of the Colorado River of the West and its tributaries*. Government Printing Office.

40. Raczkowski, W., Wójcik, A., & Zuchiewicz, W. (1984). Late Neogene–Quaternary tectonics of the Polish Carpathians in the light of neotectonic mapping. *Tectonophysics, 108*(1-2), 51–69. https://doi.org/10.1016/0040-1951(84)90230-2

41. Saint-Marc, P. (1972). Le Crétacé inférieur et moyen du bord occidental du Jabal Sannine (Liban). *Notes et Mémoires sur le Moyen-Orient, 12*, 217–226.

42. Saint-Marc, P. (1974). Étude stratigraphique et micropaléontologique de l'Albien, du Cénomanien et du Turonien du Liban. *Notes et Mémoires sur le Moyen-Orient, 13*, 8–342.

43. Smith, A. G., Smith, D. G., & Funnell, B. M. (1994). *Atlas of Mesozoic and Cenozoic coastlines*. Cambridge University Press.

44. Stearns, R. G. (1967). Warping of the Western Highland Rim Peneplain in Tennessee by groundwater sapping. *Geological Society of America Bulletin, 78*(9), 1111–1124. https://doi.org/10.1130/0016-7606(1967)78[1111:WOWHRP]2.0.CO;2

45. Strahler, A. N. (1952). Hypsometric (area-altitude) analysis of erosional topography. *Geological Society of America Bulletin, 63*(11), 1117–1142. https://doi.org/10.1130/0016-7606(1952)63[1117:HAOAET]2.0.CO;2

46. Svensson, H. (1950). *Method for exact characterizing of denudation surfaces, especially peneplains, as to the position in space* (Lund Studies in Geography, Series A, No. 8). Stockholm.

47. Ufintsev, G., Alekseenko, S., & Onukhov, F. (2009). Morphotectonics of the Lower Amur region. *Russian Journal of Pacific Geology, 3*(6), 585–595. https://doi.org/10.1134/S1819714009060062

48. Unwin, D. (1975). *An introduction to trend surface analysis* (CATMOG No. 5). Geo Abstracts. https://www.researchgate.net/publication/249001306

49. Veevers, J. J., & Morgan, P. (2000). *Billion-year Earth history of Australia and neighbors in Gondwanaland*. GEMOC Press.

50. Zuchiewicz, W., & Oszczypko, N. (2008). The topography of the Magura floor thrust and morphotectonics of the outer West Carpathians in Poland. *Annales Societatis Geologorum Poloniae, 78*, 135–149. http://www.asgp.pl/sites/default/files/volumes/78_2_135_149.pdf

DOI: 10.5281/zenodo.19107119